房腫大の程度と発症時期、性腺機能不全の程度、内分泌学的検査データ、アロマターゼ阻害剤の効果について検討した。

（倫理面への配慮）

本研究は、ヒトゲノム・遺伝子解析研究に関する倫理指針（平成16年文部科学省・厚生労働省・経済産業省告示第1号）を遵守して施行した。本課題は、国立成育医療研究センターおよび千葉大学の倫理委員会において承認されている。臨床検体は、患者本人または両親から書面でのインフォームドコンセントを得たのちに採取した。検体は、各医療機関で個人識別情報をなくして匿名化された後に当研究機関に送付された。

C．研究結果

1．新規患者の遺伝子解析

4例において、CYP19A1周辺のゲノム構造異常を同定した。1例はCYP19A1プロモーターを包含する微小重複、1例は隣接遺伝子DMXL2エクソンの一部を包含する微小欠失であった。これらは、われわれがこれまでに同定した家系と同様の異常であると推測される。一方、他の2例では、それぞれCYP19A1周辺の逆位と重複を伴う複雑構造異常とCYP19A1翻訳領域を包含する重複が同定された（図1）。

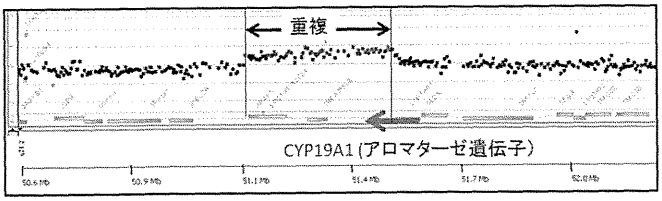

切断点周辺の塩基配列決定では、遺伝性女性化乳房を招くゲノム微細異常が、反復配列依存性および非依存性の両者の機序によって生じることが明確となった。すなわち、DXML2の一部を包含する微小欠失は反復配列間の非相同組換え（Non-allelic homologous recombination (NAHR)）もしくはDNA切断に起因するNon-homologous end-joining (NHEJ)によって生じ、プロモーターの重複と複雑構造常は、DNA複製時のエラーに起因するmicrohomologyを介したfork stalling and template switching（FoSTes）によって生じる可能性が高いことが見出された。

2．遺伝子型—表現型解析

16名の患者の解析から、ゲノム異常と疾患重症度の関連が明確となった（添付資料1）。（1）患者の乳房腫大と骨年齢促進の程度には、明瞭な症例間差異が存在する。（2）重複陽性患者では、乳房腫大が比較的軽度であり、発症時期が遅い。また、最終身長は正常範囲内である。（3）逆位陽性患者は、思春期前に発症する重度の乳房腫大と著明な骨年齢の促進、最終身長の低下によって特徴づけられる。（4）欠失陽性患者では、中等度の臨床症状が認められる。（5）全例において、FSH優位のゴナドトロピン分泌不全とそれに伴う比較的軽度な性腺機能不全が認められる。ゴナドトロピン分泌障害の程度は、ゲノム異常のパターンに無関係である。（6）男性患者では、妊孕性は保持される。（7）アロマターゼ阻害剤（Anastrozole）は、本症の治療に有用である。重複および欠失陽性例では1 mg/ 日、逆位陽性例では2-4 mg/ 日のAnastrozole1の投与によって明確な臨床症状と内分泌所見の改善が確認された。

D．考察

1．新規患者の遺伝子解析

遺伝性女性化乳房の発症には、CYP19A1遺伝子周辺の多様な染色体微細構造異常が関与することが明確となった。本症患者におけるCYP19A1過剰発現の原因として、遺伝子翻訳領域の重複、プロモーター数の増加、広範囲発現遺伝子とのキメラ遺伝子の形成の3つが存在することが見出された。なお、このようなゲノム構造異常の発症には、NAHR,NHEJ、FoSTesなどさまざまな要因が関与すると推測される。このことから、15番染色体長腕には、ゲノム脆弱性を惹起する何らかの配列モチーフが存在する可能性が示唆される。

これまで遺伝子過剰発現に起因する先天性疾患のなかで、その発症機序が解明されているものは少数にとどまる。本症の分子遺伝学的基盤の解明は、ヒトのゲノム病の成立機序の理解に貢献すると期待される。

2. 遺伝子型—表現型解析

本症の乳房腫大と骨年齢促進の重症度は、ゲノム異常の種類に相関することが明確となった。このことは、本症の重症度が、CYP19A1 に結合したプロモーターの機能と構造を反映することを示唆する。すなわち、生理的CYP19A1プロモーターの重複は、通常のCYP19A1発現部位に限局した過剰発現を招くため、比較的少量のアロマターゼ蛋白過剰産生を招くと推測される。一方、欠失例と逆位例のキメラ遺伝子形成には広範囲発現遺伝子のプロモーターが関与するため、多量のアロマターゼ蛋白が産生されると予想される。さらに、DMXL2 エクソン 1 には翻訳開始コドンが存在するため、DMXL2-CYP19A1 キメラ遺伝子は、アロマターゼ蛋白のほかに DMXL2 翻訳開始コドンから読みとられる無機能蛋白をコードするが、エクソン 1 に翻訳開始コドンを持たない逆位例のキメラ遺伝子ではアロマターゼ蛋白のみが産生される。このようなプロモーター構造の違いが、欠失陽性患者と逆位陽性患者の重症度の差に寄与している可能性がある。事実、5'-RACE 産物のなかでキメラ mRNA の占める割合は、欠失例では数%であるのに対し、既報の逆位例では 80-90%であった。

一方、ゴナドトロピン分泌障害の程度がゲノム異常のパターンに無関係であったことからは、比較的軽度の循環血中エストロゲン増加が、強い FSH 抑制作用を発揮することが示唆される。これまでエストロゲンが視床下部-下垂体-性腺系に対し抑制的に働くことが知られていたが、その作用点は不明であった。今回の成績は、エストロゲンフィードバックの主な作用点が、下垂体における FSH の分泌抑制であることを明確とするものである。また、本研究では、アロマターゼ阻害剤の有効性が確認された。早期診断とアロマターゼ阻害剤による治療は、本症の予後の改善に役立つと期待される。

E. 結論

遺伝性女性化乳房の発症に、NAHR、NHEJ、FoSTes に起因する CYP19A1 遺伝子周辺の染色体微細構造異常が関与することが明確となった。また、本症の臨床症状の一部はゲノム異常の種類に相関するが、ゴナドトロピン分泌障害の程度は全患者で同等であることから、比較的軽度の循環血中エストロゲン増加が下垂体における FSH を強く抑制することが見出された。アレイ CGH を用いた早期診断とアロマターゼ阻害剤による治療は、本症の予後の改善に役立つと期待される。

F. 健康危険情報

なし

G. 研究発表

1. 論文発表

1. Fukami M, Shozu M. Ogata T. Molecular Bases and Phenotypic Determinants of Aromatase Excess Syndrome. Int J Endocrinol. 584807.2012
2. 深見真紀、緒方勤. 小児内分泌疾患とゲノムコピー数異常　生体の科学 62 (6) 546-551　2011.
3. 深見真紀、曽根田瞬、加藤芙弥子、花木啓一、神埼晋、大山建司、佐野友昭、西垣敏紀、稲垣朱実、高木博史、Gerhard binder、横谷進、堀川玲子、生水真紀夫、緒方勤. 遺伝性女性化乳房症 6 家系における疾患成立機序と臨床像の解明. 臨床内分泌 Update proceedings.2011 June; 87(Supplement): 94-97

2. 講演・シンポジウム

1. 深見真紀.　PORD Update. スプリングセミナー2011.　2011 年 5 月 27–29 日、大阪
2. 深見真紀. 先天性内分泌異常症を招くゲノム微細構造異常：CGH 解析による新たな疾患成立機序の解明。アジレントゲノミクスフォーラム 2011 年 6 月 14 日、東京
3. 深見真紀. 小児内分泌疾患診療に役立つ分子遺伝学の知識　第 45 回　小児内分泌学会学術集会教育セミナー　2011 年 10 月 6 日、大宮
4. 深見真紀.　小児内分泌疾患の分子遺伝学：最近の進歩と今後の展望　静岡県小児内分泌学術講演会　2011 年 12 月 1 日、浜松
5. 深見真紀. チトクロームP450 オキシドレダクターゼ（POR）異常症の分子基盤：　POR 遺伝子発現制御機構の解明 第１６回生殖内分泌学会学術集会シンポジウム 2011 年 11 月 19 日、東京
6. Fukami M, Shozu M, Soneda S, Kato F, Inagaki A, Takagi H, Hanaki K, Kanzaki S, Ohyama K, Sano T, Nishigaki T, Yokoya S, Binder G, Horikawa R, Ogata T. Aromatase Excess Syndrome Caused by Cryptic Duplications and Deletions Leading to

Gain-of-Function of CYP19A1. ENDO annual meeting, June 4-7, 2011, Boston

7. Soneda S, Fukami M, Ogata T. Identification of the Promoter Region for Cytochrome P450 Oxidoreductase Gene. ENDO annual meeting, June 4-7, 2011,Boston
8. Fukami M, Shozu M, Soneda S, Kato F, Inagaki A, Takagi H, Hanaki K, Kanzaki S, Ohyama K, Sano T, Nishigaki T, Yokoya S, Binder G, Horikawa R, Ogata T. Aromatase excess syndrome: identification of cryptic duplications and deletions leading to gain-of-function of CYP19A1 and assessment of phenotypic determinants. 50th annual ESPE meeting, 25-28 September, 2011, Glasgow
9. Ogata T, Soneda S, Fukami M. Identification and characterization of the promoter region for cytochrome P450 oxidoreductase gene. 50th annual ESPE meeting, 25-28 September, 2011, Glasgow

H. 知的財産権の出願・登録状況

1. 特許取得

なし

2. 実用新案登録

なし

3. その他

なし

表 1. これまでに報告されたアロマターゼ過剰症患者の遺伝子異常と臨床所見

遺伝子異常	微小重複	微小欠失	染色体逆位
症例数	2家系4例	4家系14例	4家系5例
獲得プロモーター[a]	*CYP19A1*	*DMXL2*	*MAPK6, CGNL1, TLN2, TMOD3*
臨床症状			
乳房腫大発症年齢 (歳)	10-13	7-11	5-8
乳房腫大重症度 (Tanner stage)	2-3	3-4	4-5
成人期身長	正常	正常	低身長
内分泌所見			
LH (基礎値)	正常	正常/低値	正常/低値
LH (GnRH負荷後[b])	正常/低値	さまざま	低値
FSH (基礎値)	低値	低値	低値
FSH (GnRH負荷後[b])	低値	低値	低値
T (基礎値)	正常/低値	正常/低値	正常/低値
T (hCG負荷後[c])	不明	正常	正常
E_1 (基礎値)	高値	高値	高値
E_2 (基礎値)	正常/高値	正常/高値	高値
E_2/T 比	高値	高値	高値
文献	(3)	(3)	(1), (2)

T: testosterone; E_1: estrone; E_2: estradiol; GnRH: gonadotropin releasing hormone; hCG: human chorionic gonadotropin

[a] *CYP19A* 1に結合しているプロモーターが本来制御している遺伝子

[b] GnRH 100 μg/m^2 (最大 100 μg) bolus i.v.; 血液採取 0, 30, 60, 90, 120分後.

[c] hCG 3000 IU/m^2 (最大5000 IU) i.m. 3日連続投与; 血液採取1日目と4日目

文献

(1) Shozu M, Sebastian S, Takayama K, Hsu WT, Schultz RA, Neely K, Bryant M, Bulun SE. Estrogen excess associated with novel gain-of-function mutations affecting the aromatase gene. N Engl J Med., 348: 1855–65, 2003

(2) Demura M, Martin RM, Shozu M, Sebastian S, Takayama K, Hsu WT, Schultz RA, Neely K, Bryant M, Mendonca BB, Hanaki K, Kanzaki S, Rhoads DB, Misra M, Bulun SE. Regional rearrangements in chromosome 15q21 cause formation of cryptic promoters for the CYP19 (aromatase) gene. Hum Mol Genet., 16: 2529–41, 2007

(3) Fukami M, Shozu M, Soneda S, Kato F, Inagaki A, Takagi H, Hanaki K, Kanzaki S, Ohyama K, Sano T, Nishigaki T, Yokoya S, Binder G, Horikawa R, Ogata T. Aromatase Excess Syndrome: Identification of Cryptic Duplications and Deletions Leading to Gain-of-Function of CYP19A1 and Assessment of Phenotypic Determinants. J Clin Endocrinol Metab. 96(6):E1035–1043, 2011

Ⅱ．診断基準案（２０１２年度版）

遺伝性女性化乳房症　診断の手引き案（2012 年度版）

遺伝性女性化乳房

遺伝性女性化乳房は、性腺外組織で過剰に産生されたエストロゲンにより男性に女性化乳房・低身長などの症状をもたらす常染色体優性の遺伝性疾患である。これまでに、アロマターゼ遺伝子に構造異常をもつ家系が知られている。アロマターゼ阻害剤投与により症状の発生を抑制できる可能性があることから、早期診断が望まれる。

診断基準

診断項目１）～４）の項目を満たすものを、臨床的に遺伝性女性化乳房と診断する。同意を得て、末梢血白血球の細胞遺伝学的検査により診断を確定する。１）～３）を満たすが、４）を満たさないものは疑い例とし、細胞遺伝学的検査により診断を確定する。血中ホルモン値は、診断の参考にとどめ、診断基準には含めない。

A. 診断項目

１）タナー分類２度以上の両側性乳房発育[注1)]

２）発症年齢が 20 歳以下[注2)]

３）２次性女性化乳房[注3)]と思春期一過性女性化乳房症[注4)]を除外できる

４）家系内発症がある[注5)]

B. 参考とする内分泌検査

- 血中エストラジオール（E2）：
  高値例が多いが、高値を示さない症例も存在する。E2 値から本症の可能性を除外することはできない。
- E2/テストステロン比：
  T から E2 への転換率を反映する。遺伝性女性化乳房症では、E2[pg/ml]/T[ng/ml](T)＞10 を示す例が多いが、その他の疾患（クラインフェルター症候群、肝疾患など）でも E2/T＞10 となることがある。
- 血中ゴナドトロピン：
  FSH 低値、LH 基準値のことが多い。
- アロマターゼ活性
  乳腺組織のアロマターゼ活性が、同年齢の健常者に比し高値を示す。乳腺以外の皮下脂肪や血中単核球のアロマターゼ活性も、高値を示す例が多い。

C. 細胞遺伝学的検査

末梢血白血球ゲノムDNAを用いてアロマターゼ遺伝子の変異を同定する[注6)]。乳腺もしくは皮膚より採取した組織から細胞を分離して、アロマターゼ活性を測定することもできる。末梢血単球で代用できることもある。

注記

注1) 乳房腫大は進行性である。腫大の程度は遺伝子型と相関しており、遺伝子変異型によっては、乳房腫大が軽度にとどまる家系もある。両側の腫大を示すが、腫大の程度に左右差がある例もある。女性例では、巨大乳房として認識される。

注2) 思春期、遅くとも20歳までに発症（乳房腫大を自覚または他覚）する。前思春期から、乳房腫大が始まる例がある。

注3) 二次性女性化乳房（付表）の可能性を除外する。二次性女性化乳房では、それぞれ原疾患の所見や兆候があるのに対し、遺伝性女性化乳房ではエストロゲン高値に基づく乳房腫大・低身長症状以外の症状を示さない。

注4) 思春期男児には、生理的な一過性両側性乳房腫大がしばしば見られる。発症時期が思春期である、症状（乳房の増大や疼痛）の進行がおおむね1年以内で止まりその後軽快に向かうなどの所見は、一過性乳房腫大を示唆する。

注5) 家系内発生があれば、本症である可能性が高い。父親に女性化乳房がみられる症例が多い。家系発生が確認できない場合でも、本症を確実に否定することはできない。母方の遺伝で巨大乳房が自覚されていない、de novoに発生した弧発例などの可能性がある。細胞遺伝学的検索、もしくは乳腺組織のアロマターゼ活性測定により診断を確定する。

注6) 5'-rapid amplification of cDNA ends, 5'RACE（プロモーター逆位）、15番染色体 comparative genomic hybridization（CGH）オリゴプローブアレイ（重複、欠失）、fluorescence in situ hybridization（FISH）等により変異を検出し、シークエンス等により確定する。

別表　女性化乳房の原因

症候性 （２次性）	A. 染色体異常	A1. Klinefelter 症候群 A2. XX 男性、Swyer 症候群 A3. その他
	B. 酵素欠損症	B1. 3β-HSD 欠損症 B2. 21-hydroxylase 欠損症 B3. 17α-hydroxylase 欠損症 B3. その他
	C. アンドロゲン 受容体関連異常症	C1. アンドロゲン不応症 C2. その他
	D. 神経筋疾患	D1. 球脊髄性筋萎縮症（Kennedy-Alter-Sung 症候群） D2. POEMS 症候群（Crow-Fukase 症候群） D3. 筋強直性ジストロフィー D4. ミトコンドリア脳筋症 D5. 筋ジストロフィー D6. その他
	E. 悪性腫瘍	E1. hCG 産生腫瘍（肺癌、胃癌、精巣腫瘍、尿路移行上皮癌など） E2. 絨毛癌（胃癌、縦隔腫瘍、膀胱癌、精巣腫瘍） E3. 胚細胞性腫瘍（精巣腫瘍、縦隔腫瘍） E4. エストロゲン産生腫瘍（胃癌、精巣腫瘍、副腎腫瘍） E5. 肝細胞癌 E6. Peutz-Jeghers 症候群 E7. 悪性リンパ腫 E8. 多発性内分泌腫瘍 E9. その他
	F. 内分泌疾患	F1. 甲状腺機能亢進症 F2. 低ゴナドトロピン性性腺機能低下症 F3. 高ゴナドトロピン血症 F4. GH 分泌不全症 F5. ACTH 単独欠損症 F6. 高プロラクチン血症 F7. その他
	G. 肝疾患	G1. 肝硬変 G2. その他
	H. 腎疾患	H1. 透析 H2. その他
	I. 薬剤性	I1. アルドステロン拮抗薬 I2. 降圧剤 I3. 抗精神薬 I4. 制酸剤 I5. ホルモン剤 I6. 抗 HIV 薬 I7. 高脂血症薬 I8. 漢方薬（牛車腎気丸） I9. 牛乳 I10. その他　(male to female などを含む)
特発性 （原発性）	J. 特定の原因が 見あたらないもの （２次性でない）	J1. 家族性・遺伝性がない J2. 家族性・遺伝性がある(推定も含む) [家系内に女性化乳房患者がいる場合など] J3. 家族歴・遺伝歴が不明 J4. その他

Ⅲ. 研究成果の刊行一覧・別刷

研究成果の刊行に関する一覧表

【雑誌】

発表者氏名	論文タイトル名	発表誌名	巻号	ページ	出版年
Maki Fukami, Junichi Suzuki, Kazuhiko Nakabayashi, Ryo Tsunashima, Tsutomu Ogata, Makio Shozu, Sinzaburo Noguchi	Lack of genomic rearrangements involving the aromatase gene *CYP19A1* in breast cancer	Breast Cancer	2013	Published online (4 pages)	2013
Fukami M, Shozu M, Ogata T	Molecular Bases and Phenotypic Determinants of Aromatase Excess Syndrome	Int J Endocrinol.	2012	584807	2012
深見真紀、曽根田瞬、加藤芙弥子、花木啓一、神埼晋、大山建司、佐野友昭、西垣敏紀、稲垣朱実、高木博史、Gerhard Binder、横谷進、堀川玲子、生水真紀夫、緒方勤	アロマターゼ過剰症６家系の分子遺伝学的/臨床的解析：新たな遺伝疾患発症機序とホルモン調節機構の解明	ホルモンと臨床	59	27-32	2012
深見真紀、緒方勤	小児内分泌疾患とゲノムコピー数異常	生体の科学	62(6)	546-551	2011
深見真紀、曽根田瞬、加藤芙弥子、花木啓一、神埼晋、大山建司、佐野友昭、西垣敏紀、稲垣朱実、高木博史、Gerhard Binder、横谷進、堀川玲子、生水真紀夫、緒方勤	遺伝性女性化乳房症6家系における疾患成立機序と臨床像の解明	臨床内分泌 Update proceedings	87(Supplement)	94-97	2011
Fukami M, Shozu M, Soneda S, Kato F, Inagaki A, Takagi H, Hanaki K, Kanzaki S, Ohyama K, Sano T, Nishigaki T, Yokoya S, Binder G, Horikawa R, Ogata T	Aromatase Excess Syndrome: Identification of Cryptic Duplications and Deletions Leading to Gain of Function of *CYP19A1* and Assessment of Phenotypic Determinants	J Clin Endocrinol Metab	96	E1035-1043	2011

発表者氏名	論文タイトル名	発表誌名	巻号	ページ	出版年
Bo Zhang, Makio Shozu, Masahiko Okada, Hiroshi Ishikawa, Tadayuki Kasai, Kouich Murakami, Kazuhito Nomura, Nobuhiro Harada, and Masaki Inoue	Insulin-Like Growth Factor I Enhances the Expression of Aromatase P450 by Inhibiting Autophagy	Endocrinology	151(10)	4949-4958	2010
生水真紀夫、碓井宏和	子宮内膜症合併不妊の治療法　10.子宮内膜症治療とアロマターゼ阻害剤	産科と婦人科	77(7)	804-811	2010

Breast Cancer
DOI 10.1007/s12282-013-0471-5

RAPID COMMUNICATION

Lack of genomic rearrangements involving the aromatase gene *CYP19A1* in breast cancer

Maki Fukami · Junichi Suzuki · Kazuhiko Nakabayashi · Ryo Tsunashima · Tsutomu Ogata · Makio Shozu · Shinzaburo Noguchi

Received: 25 February 2013 / Accepted: 15 April 2013

Abstract Increased intratumoral expression of aromatase, the key enzyme for estrogen biosynthesis, is predicted to be of critical importance in the development of breast cancer. Recently, several germline rearrangements at 15q21 have been shown to cause overexpression of the aromatase gene *CYP19A1* and resulting aromatase excess syndrome. To determine whether submicroscopic genomic rearrangements at 15q21 are involved in aromatase overexpression in breast cancer tissues, we investigated copy-number alterations in genomic DNA obtained from 44 tumor samples. Comparative genomic hybridization analysis identified no deletion or duplication at 15q21 in the 44 samples. These results, in conjunction with previous data, indicate that aromatase overexpression in breast cancer tissues is likely to result from a promoter switch of *CYP19A1* and/or accumulation of *CYP19A1*-expressing cells, rather than from cryptic transactivation of *CYP19A1* because of genomic rearrangements at 15q21.

Keywords Breast cancer · Aromatase · *CYP19A1* · Gene expression · Genomic rearrangement

Abbreviations
AEXS Aromatase excess syndrome
CGH Comparative genomic hybridization

Introduction

Estrogens stimulate the proliferation of breast cancer cells, possibly by transactivating growth factor genes or oncogenes [1, 2]. Although estrogens are usually synthesized in a variety of tissues, including ovaries, skin, and fat, they can also be produced locally in breast cancer tissues [1, 3, 4]. Previous studies have revealed enhanced expression of aromatase, the key enzyme for estrogen biosynthesis, in breast cancer epithelial cells and in immature fibroblasts around the malignant cells [1, 4, 5]. Aromatase overexpression in breast cancer tissues is predicted to be critically important in tumor development [1, 5].

Recently, we and other groups have described an autosomal dominant disorder referred to as aromatase excess syndrome (AEXS), which is characterized by gynecomastia resulting from increased expression of the aromatase gene *CYP19A1* [6–8]. The molecular bases of AEXS include tandem duplications at 15q21.2 involving the promoter region of *CYP19A1* and a variety of deletions and

M. Fukami (✉) · J. Suzuki · T. Ogata
Department of Molecular Endocrinology, National Research Institute for Child Health and Development, 2-10-1 Okura, Setagaya, Tokyo 157-8535, Japan
e-mail: fukami-m@ncchd.go.jp

J. Suzuki
Department of Pediatrics and Child Health, Nihon University School of Medicine, Tokyo, Japan

K. Nakabayashi
Department of Maternal-Fetal Biology, National Research Institute for Child Health and Development, Tokyo, Japan

R. Tsunashima · S. Noguchi
Department of Breast and Endocrine Surgery, Osaka University Graduate School of Medicine, Osaka, Japan

T. Ogata
Department of Pediatrics, Hamamatsu University School of Medicine, Hamamatsu, Japan

M. Shozu
Department of Reproductive Medicine, Graduate School of Medicine, Chiba University, Chiba, Japan

Published online: 30 April 2013

Table 1 Breast cancer samples examined in this study

Sample	ER[a]	PR[a]	HER2[b]	Menopausal status	Age (years)
1	Positive	Positive	Negative	Postmenopausal	78
2	Positive	Positive	Negative	Postmenopausal	63
3	Positive	Positive	Negative	Postmenopausal	51
4	Positive	Positive	Negative	Postmenopausal	56
5	Positive	Positive	Negative	Postmenopausal	55
6	Positive	Positive	Negative	Postmenopausal	65
7	Positive	Positive	Negative	Postmenopausal	58
8	Positive	Positive	Negative	Postmenopausal	71
9	Positive	Positive	Negative	Postmenopausal	64
10	Positive	Positive	Negative	Postmenopausal	66
11	Positive	Positive	Negative	Postmenopausal	59
12	Positive	Positive	Negative	Postmenopausal	81
13	Positive	Positive	Negative	Postmenopausal	61
14	Positive	Positive	Negative	Postmenopausal	68
15	Positive	Positive	Negative	Postmenopausal	65
16	Negative	Negative	Negative	Postmenopausal	67
17	Negative	Negative	Negative	Premenopausal	49
18	Negative	Negative	Positive	Postmenopausal	68
19	Negative	Negative	Negative	Postmenopausal	70
20	Negative	Negative	Positive	Premenopausal	42
21	Positive	Positive	Negative	Postmenopausal	73
22	Positive	Positive	Negative	Postmenopausal	56
23	Positive	Positive	Negative	Postmenopausal	56
24	Positive	Positive	Negative	Postmenopausal	57
25	Positive	Positive	Negative	Postmenopausal	56
26	Positive	Positive	Negative	Postmenopausal	70
27	Positive	Positive	Negative	Postmenopausal	71
28	Positive	Positive	Negative	Postmenopausal	80
29	Positive	Positive	Negative	Postmenopausal	60
30	Positive	Positive	Negative	Postmenopausal	80
31	Positive	Positive	Negative	Postmenopausal	72
32	Positive	Positive	Negative	Postmenopausal	64
33	Positive	Positive	Negative	Postmenopausal	65
34	Positive	Positive	Negative	Postmenopausal	80
35	Positive	Positive	Negative	Postmenopausal	59
36	Positive	Positive	Negative	Postmenopausal	60
37	Positive	Positive	Negative	Postmenopausal	62
38	Positive	Positive	Negative	Postmenopausal	63
39	Positive	Positive	Negative	Postmenopausal	58
40	Positive	Positive	Negative	Postmenopausal	69
41	Positive	Positive	Negative	Postmenopausal	65
42	Positive	Positive	Negative	Postmenopausal	70
43	Positive	Positive	Negative	Postmenopausal	62
44	Positive	Positive	Negative	Postmenopausal	69

ER estrogen receptor; *PR* progesterone receptor; *HER2* human epidermal growth factor receptor 2

[a] ER and PR were analyzed by use of immunohistochemical assays. The results were defined as positive when more than 10 % of the tumor cells were positively stained

[b] HER2 amplification was analyzed by fluorescence in situ hybridization analysis. Signal intensities >2.0 were assessed as positive

inversions at 15q21.1-21.3 that create chimeric genes consisting of coding exons of *CYP19A1* and the promoter-associated exons of other genes. Identification of highly heterogeneous rearrangements in patients with AEXS indicates that the chromosomal region around *CYP19A1* is particularly vulnerable to genomic abnormalities [8]. Therefore, submicroscopic rearrangements at 15q21 generated in germ cells or in somatic cells may underlie

aromatase overexpression in breast cancer tissues. Here, we performed copy-number analysis of the 15q21 region in 44 genomic DNA samples obtained from breast cancer tissues.

Materials and methods

Tumor tissue samples

This study was approved by the Institutional Review Board Committees at Osaka University and the National Center for Child Health and Development. After obtaining written informed consent, breast cancer tissues were obtained at surgery from 44 Japanese females aged 42–80 years (Table 1). The samples were frozen in liquid nitrogen. All 44 tumors were invasive ductal carcinoma. The samples were examined for levels of expression of estrogen receptor and progesterone receptor, and for amplification of human epidermal growth factor receptor 2, as described elsewhere [9] (Table 1).

Comparative genomic hybridization analysis

Genomic DNA was extracted from tumor tissues by use of a DNeasy blood and tissue kit (Qiagen, Maryland, USA). The DNA samples were subjected to comparative genomic hybridization (CGH) analyses by use of a custom-made oligoarray (8 × 60 k format; Agilent Technologies, Palo Alto, CA, USA). The array contained approximately 16,000 probes for the 1.5 Mb region at 15q21 (chr15:51,000,000–52,500,000; hg 19, build 37), together with several reference probes for other genomic regions. The procedure was conducted in accordance with the manufacturer's instructions. A genomic DNA sample obtained from leukocytes of an unaffected Japanese 58-year-old female was used as a control.

Results

CGH analysis

Comparative genomic hybridization analysis indicated a normal copy-number for exons 1–10 of *CYP19A1* in the 44 samples (Fig. 1a). Furthermore, no deletion or duplication was detected in the 1.5 Mb genomic region at 15q21 (Fig. 1a).

Discussion

Comparative genomic hybridization analysis identified no copy-number alterations at 15q21 in 44 breast cancer tissues. It is worth remarking that the method used in this

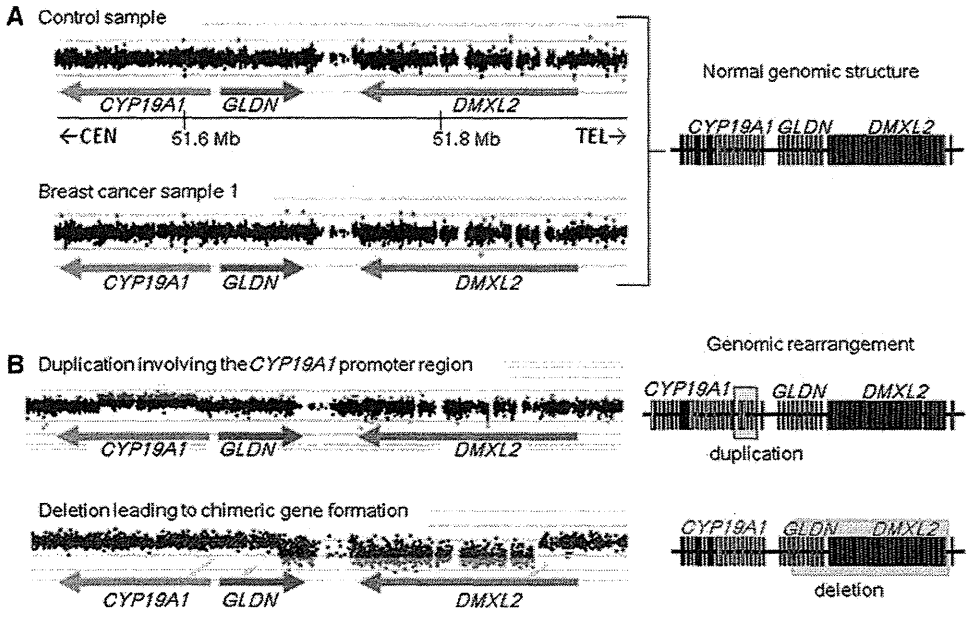

Fig. 1 **a** Comparative genomic hybridization (CGH) analysis (*left panel*) and schematic representation of the normal genomic structure in the control and breast cancer samples (*right panel*). The *black*, *red*, and *green dots* denote signals indicative of normal, increased (>+0.5), and reduced (<−1.0) copy-numbers, respectively. The *arrows* indicate genomic positions of *CYP19A1*, *GLDN*, and *DMXL2* (5′ → 3′). The positions correspond to the human genome reference assembly (UCSC genome browser, February 2009, hg19, build 37). **b** Genomic abnormalities previously identified in patients with aromatase excess syndrome. These germline rearrangements have been implicated in *CYP19A1* overexpression [8]. The results of CGH analysis (*left panel*) and schematic representation of the rearranged genome (*right panel*) are shown

study is capable of identifying all the duplications and deletions that have previously been associated with AEXS (Fig. 1b) [8], although copy-number-neutral inversions may not be detected by CGH analysis. These results imply that copy-number gains of *CYP19A1* and formation of chimeric genes arising from cryptic rearrangements are not the major factors underlying aromatase overexpression in breast cancer tissues. Furthermore, lack of genomic rearrangements in the 15q21 region in the 44 samples suggests that this region would not be a hotspot for somatic rearrangements, especially considering that breast cancer tissues are characterized by prominent genomic instability [10].

Previous studies have attributed aromatase overexpression in breast cancer tissues to alternative use of the non-coding exons 1 of *CYP19A1* [5, 11]. Of the 11 exons 1, exons 1.3, II, and 1.7 were found to predominantly control expression of *CYP19A1* in breast cancer tissues, whereas exon 1.4 functioned as the major promoter in normal breast tissues. This promoter switch seemed to result from the perturbed production of signal molecules in tumor tissues. For example, overproduction of prostaglandins has been associated with activation of exons 1.3 and II [1, 5, 11]. Furthermore, accumulation of immature adipose fibroblasts with strong expression of *CYP19A1* has also been proposed to contribute to aromatase excess in breast cancer tissues [5].

It should be noted that our conclusion is based on results from 44 samples only. Furthermore, *CYP19A1* mRNA levels were not analyzed in this study. In this regard, it is known that although increased aromatase activity is a common feature in breast cancer tissues, mRNA levels of *CYP19A1* vary among samples [12, 13]. Therefore, the absence of genomic rearrangements in our 44 samples may be ascribed to low expression of *CYP19A1* in these tissues. Indeed, genomic rearrangements at 15q21 may be hidden in a specific group of breast cancers with overexpression of *CYP19A1*. Further CGH and mRNA analysis for several tumor samples is necessary to clarify the presence or absence of an association between genomic rearrangements at 15q21 and intratumoral estrogen overproduction.

In summary, this study, in conjunction with previous data, implies that aromatase overexpression in breast cancer tissues is likely to result from a promoter switch of *CYP19A1* induced by trans-acting factors and/or accumulation of *CYP19A1*-expressing cells, rather than from cryptic transactivation of *CYP19A1* because of genomic rearrangements at 15q21.

Acknowledgments This work was supported by the Grant-in-Aid for Scientific Research on Innovative Areas (22132004) from the Ministry of Education, Culture, Sports, Science and Technology, by the Grant-in-Aid for Scientific Research (B) (23390249) from the Japan Society for the Promotion of Science, by the Grant for Research on Intractable Diseases from the Ministry of Health, Labor and Welfare, and by the Grants from National Center for Child Health and Development, from Takeda foundation, and from Daiichi-Sankyo Foundation of Life Science.

Conflict of interest The authors declare that no conflict of interests exists.

References

1. Bulun SE, Lin Z, Imir G, Amin S, Demura M, Yilmaz B, et al. Regulation of aromatase expression in estrogen-responsive breast and uterine disease: from bench to treatment. Pharmacol Rev. 2005;57:359–83.
2. Kulendran M, Salhab M, Mokbel K. Oestrogen-synthesising enzymes and breast cancer. Anticancer Res. 2009;29:1095–109.
3. Bulun SE, Chen D, Lu M, Zhao H, Cheng Y, Demura M, et al. Aromatase excess in cancers of breast, endometrium and ovary. J Steroid Biochem Mol Biol. 2007;106:81–96.
4. Sasano H, Miki Y, Nagasaki S, Suzuki T. In situ estrogen production and its regulation in human breast carcinoma: from endocrinology to intracrinology. Pathol Int. 2009;59:777–89.
5. Bulun SE, Lin Z, Zhao H, Lu M, Amin S, Reierstad S, et al. Regulation of aromatase expression in breast cancer tissue. Ann N Y Acad Sci. 2009;1155:121–31.
6. Demura M, Martin RM, Shozu M, Sebastian S, Takayama K, Hsu WT, et al. Regional rearrangements in chromosome 15q21 cause formation of cryptic promoters for the CYP19 (aromatase) gene. Hum Mol Genet. 2007;16:2529–41.
7. Shozu M, Sebastian S, Takayama K, Hsu WT, Schultz RA, Neely K, et al. Estrogen excess associated with novel gain-of-function mutations affecting the aromatase gene. N Engl J Med. 2003;348:1855–65.
8. Fukami M, Shozu M, Soneda S, Kato F, Inagaki A, Takagi H, et al. Aromatase excess syndrome: identification of cryptic duplications and deletions leading to gain of function of CYP19A1 and assessment of phenotypic determinants. J Clin Endocrinol Metab. 2011;96:E1035–43.
9. Naoi Y, Kishi K, Tanei T, Tsunashima R, Tominaga N, Baba Y, et al. Development of 95-gene classifier as a powerful predictor of recurrences in node-negative and ER-positive breast cancer patients. Breast Cancer Res Treat. 2011;128:633–41.
10. Fridlyand J, Snijders AM, Ylstra B, Li H, Olshen A, Segraves R, et al. Breast tumor copy number aberration phenotypes and genomic instability. BMC Cancer. 2006;6:96.
11. Khan SI, Zhao J, Khan IA, Walker LA, Dasmahapatra AK. Potential utility of natural products as regulators of breast cancer-associated aromatase promoters. Reprod Biol Endocrinol. 2011;9:91.
12. Bulun SE, Price TM, Aitken J, Mahendroo MS, Simpson ER. A link between breast cancer and local estrogen biosynthesis suggested by quantification of breast adipose tissue aromatase cytochrome P450 transcripts using competitive polymerase chain reaction after reverse transcription. J Clin Endocrinol Metab. 1993;77:1622–8.
13. Bulun SE, Simpson ER. Breast cancer and expression of aromatase in breast adipose tissue. Trends Endocrinol Metab. 1994;5:113–20.

Hindawi Publishing Corporation
International Journal of Endocrinology
Volume 2012, Article ID 584807, 8 pages
doi:10.1155/2012/584807

Review Article

Molecular Bases and Phenotypic Determinants of Aromatase Excess Syndrome

Maki Fukami,[1] Makio Shozu,[2] and Tsutomu Ogata[1,3]

[1] *Department of Molecular Endocrinology, National Research Institute for Child Health and Development, 2-10-1 Ohkura, Setagaya, Tokyo 157-8535, Japan*
[2] *Department of Reproductive Medicine, Graduate School of Medicine, Chiba University, 1-8-1 Inohana, Chuo-ku, Chiba City 206-8670, Japan*
[3] *Department of Pediatrics, Hamamatsu University School of Medicine, 1-20-1 Handayama, Higashi-ku, Shizuoka, Hamamatsu 431-3192, Japan*

Correspondence should be addressed to Maki Fukami, mfukami@nch.go.jp

Received 9 July 2011; Revised 22 September 2011; Accepted 2 October 2011

Academic Editor: Rodolfo Rey

Aromatase excess syndrome (AEXS) is a rare autosomal dominant disorder characterized by gynecomastia. This condition is caused by overexpression of *CYP19A1* encoding aromatase, and three types of cryptic genomic rearrangement around *CYP19A1*, that is, duplications, deletions, and inversions, have been identified in AEXS. Duplications appear to have caused *CYP19A1* overexpression because of an increased number of physiological promoters, whereas deletions and inversions would have induced wide *CYP19A1* expression due to the formation of chimeric genes consisting of a noncoding exon(s) of a neighboring gene and *CYP19A1* coding exons. Genotype-phenotype analysis implies that phenotypic severity of AEXS is primarily determined by the expression pattern of *CYP19A1* and the chimeric genes and by the structural property of the fused exons with a promoter function (i.e., the presence or the absence of a natural translation start codon). These results provide novel information about molecular mechanisms of human genetic disorders and biological function of estrogens.

1. Introduction

Aromatase encoded by *CYP19A1* is a cytochrome P450 enzyme that plays a key role in estrogen biosynthesis [1]. It catalyzes the conversion of Δ^4-androstendione into estrone (E_1) and that of testosterone (T) into estradiol (E_2) in the placenta and ovary as well as in other tissues such as the fat, skin, bone, and brain [1].

Overexpression of *CYP19A1* causes a rare autosomal dominant disorder referred to as aromatase excess syndrome (AEXS, OMIM no. 139300) [2–8]. AEXS is characterized by pre- or peripubertal onset gynecomastia, gonadal dysfunction, advanced bone age from childhood to pubertal period, and short adult height in affected males [2–8]. In particular, gynecomastia is a salient feature in AEXS, and, therefore, this condition is also known as hereditary gynecomastia or familial gynecomastia [5]. Affected females may also show several clinical features such as macromastia, precocious puberty, irregular menses, and short adult height [5, 6, 8].

Recently, three types of cryptic genomic rearrangements around *CYP19A1* have been identified in 23 male patients with AEXS [2–4]. The results provide useful implications not only for the clarification of underlying mechanisms but also for the identification of phenotypic determinants. Here, we review the current knowledge about AEXS.

2. The Aromatase Gene (*CYP19A1*)

CYP19A1 encoding aromatase is located on 15q21.2 adjacent to *DMXL2* and *GLDN* (Figure 1) [3, 9]. It spans ~123 kb and consists of at least 11 noncoding exons 1 and nine coding exons 2–10 [9–12]. Each exon 1 is accompanied by a tissue-specific promoter and is spliced alternatively onto a common splice acceptor site at exon 2, although some transcripts are known to contain two of the exons 1 probably due to a splice error [9–11]. Transcription of *CYP19A1* appears to be tightly regulated by alternative usage of the multiple

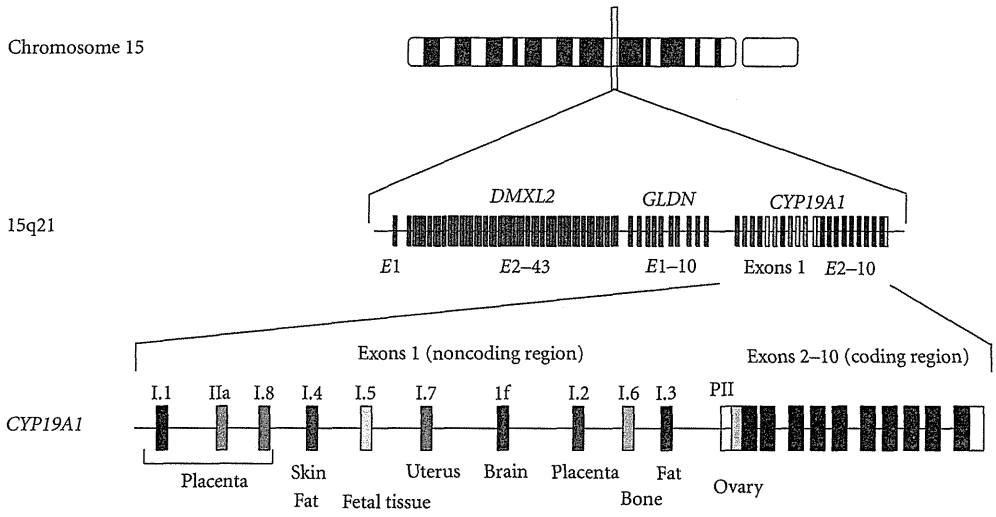

FIGURE 1: Simplified schematic representation indicating the genomic structure of *CYP19A1*. *CYP19A1* is located on 15q21.2 adjacent to *DMXL2* and *GLDN* and consists of at least 11 noncoding exons 1 and nine coding exons 2–10 [9, 10]. Each exon 1 is accompanied by a tissue-specific promoter and is spliced alternatively onto a common splice acceptor site at exon 2 [9–13].

promoters [9–13]. Actually, *CYP19A1* is strongly expressed in the placenta and moderately expressed in the ovary, whereas it is only weakly expressed in a rather limited number of tissues including skin, fat, and hypothalamus [4, 13]. Of the 11 noncoding exons 1, exon I.4 seems to play a critical role in the regulation of estrogen biosynthesis in males, because this exon contains the major promoter for extragonadal tissues [9, 10].

3. Molecular Bases of AEXS

A family with dominantly transmitted gynecomastia of prepubertal onset was first described in 1962 by Wallach and Garcia [14]. After this initial report, several cases have been described [5–8, 15]. Laboratory examinations of the affected males revealed markedly elevated serum estrogen values and estrogen/androgen ratios and significantly increased aromatase activity in fibroblasts and lymphocytes [5–8, 15]. Linkage analyses in two families indicated a close association between *CYP19A1*-flanking polymorphic markers and the disease phenotype [5, 6]. Thus, the condition was assumed to be caused by gain-of-function mutations of *CYP19A1*, and, therefore, the name of AEXS was coined for this condition [7, 8]. However, since direct sequencing and Southern blotting analysis failed to detect mutations or copy number abnormalities in the coding region of *CYP19A1* [5, 6], the molecular basis of this entity remained elusive until recently.

In 2003, Shozu et al. reported a father-son pair and a sporadic case with AEXS in whom they identified heterozygous chromosomal inversions of the chromosome 15 [2]. Subsequently, Demura et al. performed detailed molecular studies for these cases and additional two cases and characterized four types of inversions affecting the 5′ region of *CYP19A1* [3]. Each inversion has resulted in the formation of a chimeric gene consisting of *CYP19A1* coding exons and exon 1 of the widely expressed neighboring genes, that is, *CGNL1*, *TMOD3*, *MAPK6*, and *TLN2*. These data imply that overexpression of *CYP19A1* in the inversion-positive cases are caused by cryptic usage of constitutively active promoters. Consistent with this, *in silico* analysis revealed the presence of promoter-compatible sequences around exon 1 of *CGN1*, *TMOD3*, and *MAPK6* in multiple cell types, although such sequences remain to be identified for noncoding exons of *TLN2* [4].

We recently studied 18 males from six families with AEXS (families A–F) and identified three types of heterozygous cryptic genomic rearrangements in the upstream region of the *CYP19A1* coding exons (Figure 2) [4]. In families A and B, we identified the same 79,156 bp tandem duplication encompassing seven of the 11 noncoding exons 1 of *CYP19A1*. Notably, this duplication includes exon I.4 that functions as a major promoter for extragonadal tissues such as fat and skin; therefore, *CYP19A1* overexpression in these families would be explained by increasing the number of this promoter. Indeed, RT-PCR analysis detected a splice variant consisting of exon I.4 at the 5′ side and exon I.8 at the 3′ side in lymphoblastoid cell lines and skin fibroblasts of the patients, indicating that the duplicated exon I.4 at the distal nonphysiological position actually functions as transcription start sites. In family C, we identified a 211,631 bp deletion affecting exons 2–43 of *DMXL2* and exons 5–10 of *GLDN*. This deletion appears to have caused *CYP19A1* overexpression because of cryptic usage of *DMXL2* exon 1 as an extra transcription start site for *CYP19A1*. Indeed, RT-PCR revealed the presence of chimeric mRNA clones consisting of *DMXL2* exon 1 and *CYP19A1* exon 2, supporting the notion that aberrant splicing has occurred between these two exons. Such *DMXL2/CYP19A1* chimeric mRNA accounted for 2–5% of *CYP19A1*-containing transcripts from skin fibroblasts. In families D–F, we identified

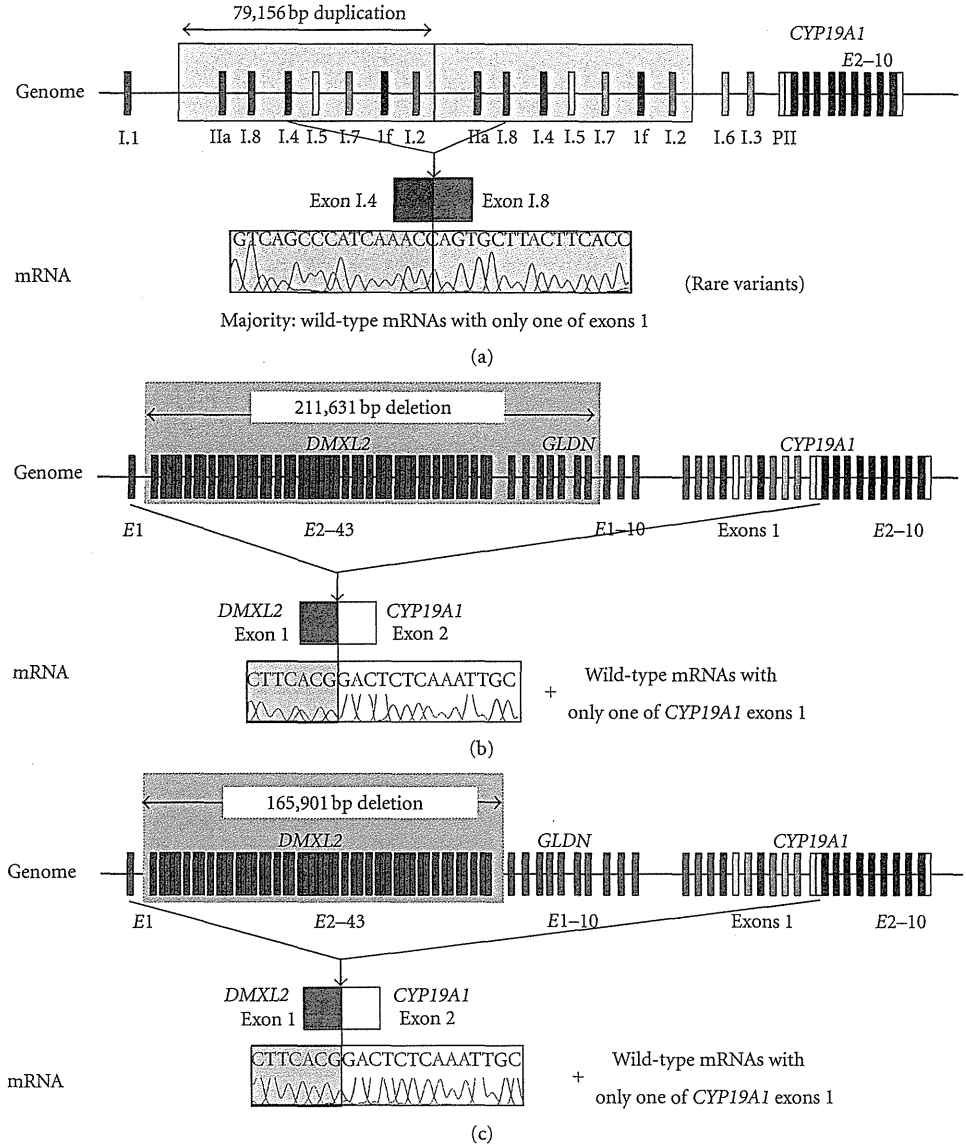

FIGURE 2: Schematic representation of duplications and deletions identified in patients with AEXS. (a) the tandem duplication of families A and B [4]. Genome: the duplication (yellow boxes) includes seven of the 11 noncoding exons 1 of *CYP19A1*. mRNA: the sequence of a rare transcript is shown. The 3′-end of exon I.4 is connected with the 5′-end of exon I.8. (b) The deletion of family C [4]. Genome: the deletion (a gray area) includes exons 2–43 of *DMXL2* and exons 5–10 of *GLDN*. mRNA: The sequence of a rare chimeric gene transcript is shown. *DMXL2* exon 1 consisting of a noncoding region and a coding region is spliced onto the common acceptor site of *CYP19A1* exon 2. (c) The deletion of families D–F [4]. Genome: the deletion (a gray area) includes exons 2–43 of *DMXL2*. mRNA: the sequence of a rare chimeric gene transcript is delineated. The mRNA structure is the same as that detected in family C.

an identical 165,901 bp deletion including exons 2–43 of *DMXL2*. RT-PCR identified the same chimeric mRNA as that detected in family C.

Collectively, three types of genomic rearrangements on 15q21 have been identified in AEXS to date, namely, inversion type (four subtypes), duplication type, and deletion type (two subtypes) (Figure 3(a)) [2–4]. In this regard, sequence analyses for the breakpoints have indicated that (1) inversion types are formed by a repeat sequence-mediated nonallelic intrachromosomal or interchromosomal recombination or by a replication-based mechanism of fork stalling and template switching (FoSTeS) that occurs in the absence of repeat sequences and is often associated with microhomology [16], (2) duplication type is generated by FoSTeS, and (3) deletions are produced by nonhomologous end joining that takes place between nonhomologous sequences and is frequently accompanied by an insertion of a short segment at the fusion point or by a nonallelic recombination [16].

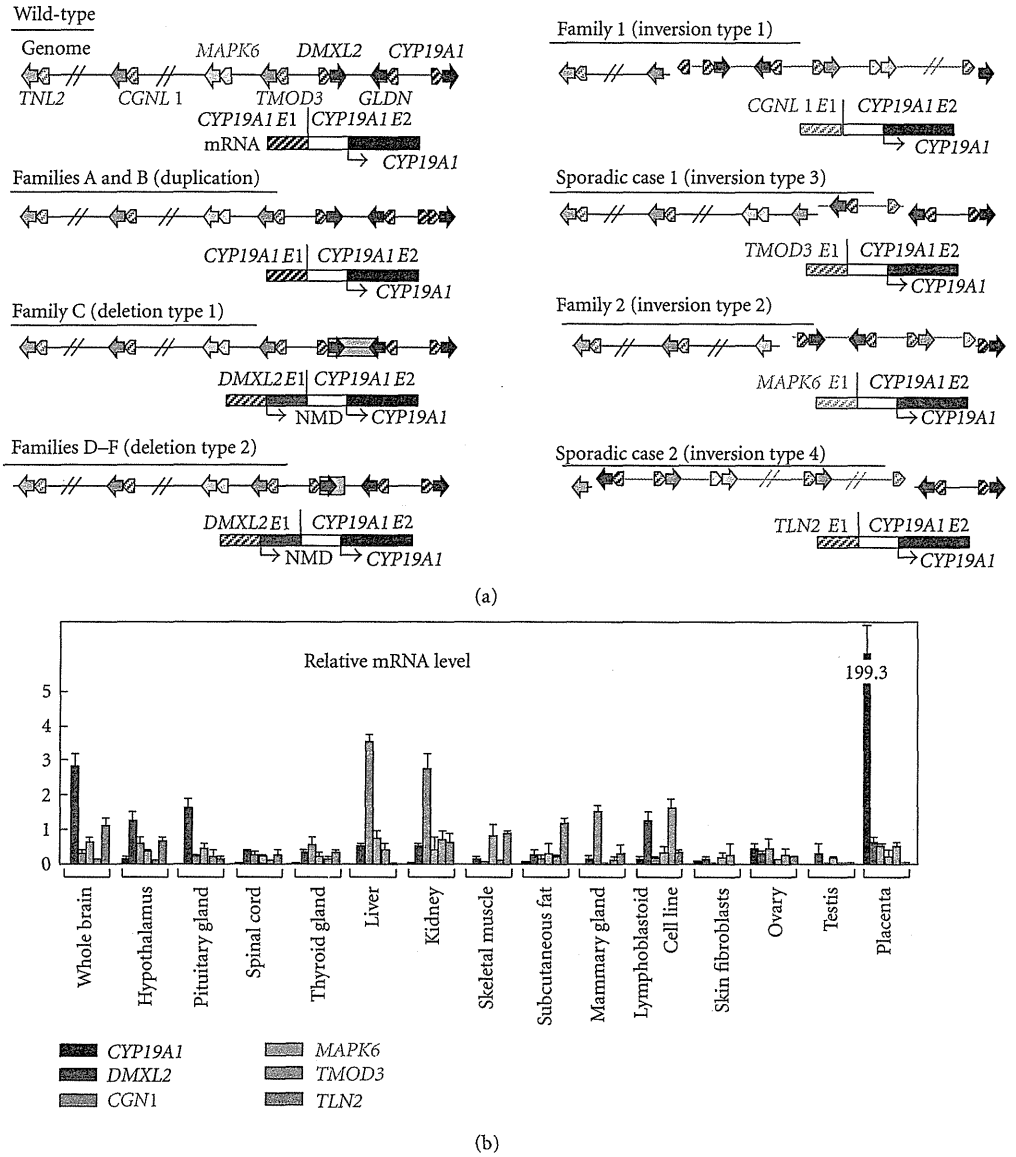

FIGURE 3: Structural and functional properties of the fused exons. (a) Schematic representation of the rearranged genome and mRNA structures. The white and the black boxes of *CYP19A1* exon 2 show untranslated region and coding region, respectively. For genome, the striped and the painted arrows indicate noncoding and coding exons, respectively (5′ → 3′). The inverted genomic regions are delineated in blue lines. For mRNA, colored striped boxes represent noncoding regions of each gene. The *DMXL2-CYP19A1* chimeric mRNA has two translation initiation codons and therefore is destined to produce not only *CYP19A1* protein but also a 47 amino acid protein which is predicted to undergo nonsense-mediated mRNA decay (NMD). The deletion and the inversion types are associated with heterozygous impairment of neighboring genes (deletion or disconnection between noncoding exon(s) and the following coding exons). The inversion subtype 1 is accompanied by inversion of eight of the 11 *CYP19A1* exons 1, and the inversion subtype 2 is associated with inversion of the placenta-specific *CYP19A1* exon I.1. (b) Expression patterns of *CYP19A1* and the five neighboring genes involved in the chimeric gene formation [4]. Relative mRNA levels against *TBP* in normal human tissues are shown.

Thus, it appears that genomic sequence around *CYP19A1* harbors particular motifs that are vulnerable to replication- and recombination-mediated errors. The results provide novel mechanisms of gain-of-function mutations leading to human diseases.

4. Clinical Features of AEXS

To date, a total of 23 male cases from 10 families have been reported to have molecularly confirmed AEXS (Table 1, Figure 3(a)) [2–4]. They exhibited pre- or peripubertal onset

Table 1: Summary of clinical studies in male patients with aromatase excess syndrome (modified from [4]).

(a)

Family			Family A			Family B		Family C				Family D			Family E	
Mutation types			Duplication			Duplication		Deletion				Deletion			Deletion	
The promoter involved in *CYP19A1* overexpression			*CYP19A1*			*CYP19A1*		*CYP19A1*				*DMXL2*			*DMXL2*	
Case		Case 1	Case 2		Case 3	Case 4		Case 5		Case 6	Case 7	Case 8		Case 9	Case 10	
Age at examination (year)		66	15		20	15		15		13	42	9		12	13	
<Phenotypic findings>																
Gynecomastia (tanner breast stage)		**2**	**2**		**2**	**3**		**4**		**4**	**4**	**3**		**4**	**4**	
Onset of gynecomastia (year)		**13**	**13**		**10**	**11**		**12**		**11**	**11**	**7**		**9**	**10**	
Mastectomy (year)		No	**Yes (15)**		No	**Yes (15)**		**Yes (15)**		**Yes (13)**	No	No		**Yes (12)**	**Yes (13)**	
Testis (ml)		N.E.	**12**		**12**	**12**		**12**		12	N.E.	3		12	20	
Pubic hair (tanner stage)		N.E.	2-3		4	5		4		3	N.E.	1		3	4	
Facial hair		Normal	Scarce		**Scarce**	Normal		Absent		Absent	N.E.	Absent		Absent	Absent	
Height (SDS)[a]		−1.2	−0.3		+0.4	+0.8		−2.0		−1.0	−1.6	**+2.7**		±0	+1.8	
Bone age (year)[b]		N.E.	N.E.		N.E.	16.0		16.0		13.5	N.E.	**13.0**		**15.0**	**17.0**	
Fertility (spermatogenesis)		Yes	?		(Yes)[h]	?		?		?	Yes	?		?	?	
<Endocrine findings>[c]		B	B	S	B	S	B	S	B	S	B	S	B	S	B	S	B	S
<At Dx>	Stimulus																	
LH (mIU/mL)	GnRH[e]	3.8	2.3	**14.3**	2.1	**17.0**	2.4	29.4	1.9	40.6	1.8	69.2	1.1	11.5	**0.6**	39.5	6.7	14.8
LH (mIU/mL)	GnRH (after priming)[f]		1.8	**9.5**	**1.3**	**10.7**												
FSH (mIU/mL)	GnRH[e]	**1.7**	**3.1**	**5.3**	**<0.5**	**1.2**	**0.9**	**2.4**	**1.4**	**4.2**	**2.0**	**7.8**	**3.2**	**6.6**	**0.6**	**2.9**	**0.7**	**1.0**
FSH (mIU/mL)	GnRH (after priming)[f]		**2.6**	**3.2**	**<0.5**	**0.9**												
Prolactin (ng/ml)			4.3		5.3				8.2		9.1		11.3		18.8			
Δ^4A (ng/mL)		**0.5**			**1.1**		**1.2**						**0.6**		**0.7**		**2.4**	2.9
T (ng/mL)	hCG[g]	2.9	**1.6**		**2.2**		4.0		**2.6**	7.2	**1.4**	7.9		**0.6**	3.6	**2.4**	3.2	9.7
DHT (ng/mL)		0.4			0.2												0.4	1.2
Inhibin B (pg/mL)		**61.6**			**74.6**		**83.5**		**75.2**									
E_1 (pg/mL)		157			120		124						57		63		53	
E_2 (pg/mL)		29	15		22		59		56		38		24	19		25	58	
E_2/T ratio ($\times 10^3$)		10.0	9.4		10.0		14.8		21.5		27.1			31.7		10.4	18.1	